Astron. Astrophys. 231, 309–326 (1990)

ASTRONOMY AND ASTROPHYSICS

Mg II quasar absorption systems and properties of gaseous haloes*

P. Petitjean and J. Bergeron

Institut d'Astrophysique de Paris, 98 bis, Boulevard Arago, F-75014 Paris, France

Received July 13, accepted September 25, 1989

Abstract. We present observations of Mg II and Fe II absorption at high spectral resolution of either 0.37 or 0.65 Å in 10 quasars. The existence of strong Mg II absorptions was a selection criterium for most objects, but our observations remain unbiased for the detection of weak Mg II doublets. Our survey has been combined with published data at similar resolution than ours, and the resulting sample comprises 33 Mg II absorption redshifts. There are groups of redshifts spanning less than a few hundred km s^{-1}, which should not be independent physical entities.

The fraction of weak to strong Mg II systems is decreasing with increasing redshift, and the evolution in redshift of the density of Mg II systems is a function of the equivalent width limit ($w_{r,\min}$) of the sample. For $w_{r,\min}$ (Mg II λ 2796) $\sim$ 0.3 Å, the redshift distribution of Mg II systems is consistent with a non evolving population as found for the Lyman limit systems. Low z weak Mg II and high z weak C IV systems should sample the same parts of gaseous halos which would then have an ionization level decreasing with decreasing redshift.

There is significant clustering of Mg II redshifts on scales up to 600 km s^{-1}. The distribution of velocity separations is best fitted by two Gaussian components with dispersions of 80 and 390 km s^{-1}. The clustering on the smaller scale could be due to relative motions of clouds within galaxy halos, that on the larger scale to relative motions of field galaxy pairs. A simple kinematical model of the absorber favors two distinct populations over a single population with two velocity distribution components.

There is a strong correlation between the total Mg II equivalent width of an absorbing entity and the number of subsystems. Most of the subcomponents have a Mg II doublet of moderate opacity, and the velocity dispersion b of some individual clouds must be larger than 10 km s^{-1}. The distribution of Mg II column densities for the observed subcomponents is fitted by a power law $dn/dN(\mathrm{Mg\,II}) \propto N(\mathrm{Mg\,II})^{-\beta}$ with $\beta = 1.0 \pm 0.1$ in the range $1\,10^{12}$ to $2\,10^{14}$ cm^{-2}.

There are one Mn II and one Ca II detections (in different absorbers) in our survey. Relative abundances of heavy elements cannot be usually estimated in low z systems except when their H I column density is very large. There is no 21 cm absorber in our sample. Using data published by Foltz et al. (1988) for the 21 cm system at $z = 0.4369$ in 3C196, we find a depletion of Ca relative to Mn of 22 implying a large dust content in this absorber.

1. Introduction

The narrow metal-rich absorption lines in quasar spectra are most likely due to low density intervening gas associated with galaxies. For lower redshift systems, current Mg II absorption line samples are compatible with intervening objects cosmologically distributed (Tytler et al., 1987; Sargent et al., 1988a) and for $z < 1$, identification of the absorbing galaxies has now been obtained in a dozen cases (Bergeron, 1988a and references therein; Bergeron and Boissé, 1989, in preparation). However, some basic properties of these large galactic gaseous envelopes are still poorly known. Only a lower limit to their overall size can be derived from available Mg II absorption line data. The Mg II samples are rest equivalent width (w_r) limited and the distribution of Mg II doublets per unit equivalent width is still sharply increasing with decreasing w_r for the current limit of available samples $w_{r,\min} = 0.25$ to 0.3Å at moderate redshift (Tytler et al., 1987; Sargent et al., 1988a). However, this may no longer be the case for Mg II systems at $z \sim 1.6$ (Lanzetta et al., 1987) for which a flattening in the distribution per unit equivalent width could be present for $w_r < 0.6$ Å. If confirmed, this would imply an evolution with redshift of the number of weak Mg II systems relative to those with $w_r \geq 0.6$ Å.

The velocity structure of Mg II absorption systems for most existing surveys is not well known for velocity separations smaller than 200 km s^{-1} due to the poor spectral resolution. There is a pronounced peak in the two-point correlation function at $\Delta v \leq$ 200 km s^{-1}(Sargent et al., 1988a) but observations at smaller Δv are necessary to find the extension of this peak towards smaller velocity separations and to determine the absorption line multiplicity.

One of our goals has been to study the velocity structure of Mg II systems at $z \sim 1$ down to $\Delta v = 30$ km s^{-1}. Our high spectral resolution observations, obtained in a large wavelength range, have also allowed to search for weak Mg II absorption doublets.

Observations in the UV are necessary to determine the ionization level and opacity to UV ionizing photons of low redshift absorbing halos. At high redshift the presence of low ionization ions is correlated to the opacity of the absorber to UV ionizing photons (Bergeron and Stasińska, 1986; Wolfe, 1986) and systems with a discontinuity at the Lyman limit are of low ionization level (Tytler, 1982; Bechtold et al., 1984; Lanzetta,

Send offprint requests to: J. Bergeron

* Based on observations made at the European Southern Observatory, La Silla, Chile

1988; Sargent et al., 1989). Observations with the Hubble Space Telescope will provide similar information for low redshift systems. At present, data obtained with the IUE satellite suggest that at least a few Mg II systems may have small H I column densities, $N(\mathrm{H\,I}) < 2\,10^{17}\mathrm{cm}^{-2}$ (Bergeron et al., 1987).

The number of Mg II systems per unit redshift shows a positive evolution with redshift (Lanzetta et al., 1987; Boulade et al. 1987; Sargent et al., 1988a), whereas surveys of Lyman limit systems (LLS) are consistent with no evolution (Bechtold et al., 1984; Lanzetta, 1988; Sargent et al., 1989). At low redshift, $z < 1$, Lyman limit systems are by far the dominant known population. At $z \sim 0.5$, Mg II systems with $w_r(\mathrm{Mg\,II}\,\lambda 2796) \geq 0.6$ Å represent only about 20% of the LLS but, at $z \sim 2$, this fraction reaches 75%. This suggests that the cosmological evolution of the density of Mg II systems per unit redshift should weaken for samples with decreasing equivalent width limit.

Two questions remain: do weak Mg II systems exist at $z \sim 2$? What is their opacity to UV ionizing photons? If the Mg II equivalent width distribution is not evolving with redshift, most of the weak systems at $z \sim 2$ should then have H I column densities smaller than $2\,10^{17}\,\mathrm{cm}^{-2}$ for consistency with the number density of LLS. Weak absorption systems at $z \sim 2$ are indeed often, if not always, optically thin to UV radiation, however they are of high ionization level with C IV present but not C II or Mg II (Boissé and Bergeron, 1985; Lanzetta et al., 1987; Sargent et al., 1988a and 1988b). This may suggest that weak systems are of low ionization level and large opacity at $z \sim 0.5$, whereas at $z \sim 2$ they are of high ionization level and optically thin to UV radiation. It is yet unclear whether systems with small Mg II or C IV equivalent widths have small column densities. Strong absorption systems are usually of high multiplicity and the line strengths roughly scale with the velocity spread of the blended narrow components (Wolfe, 1986; York et al., 1986). Using our high resolution data, we can search for correlations between the total equivalent widths of the blends and the multiplicity of the systems, and between the equivalent widths of individual components and their column densities.

The observations are described in Sect 2. The results of our search for weak Mg II systems at $z \sim 1$ are given in Sect 3 and they are compared with those from previous surveys. In Sect 4 we discuss the clustering of Mg II absorbers. We investigate the relationships between line equivalent widths, multiplicity and column densities in Sect 5. We estimate ionic abundances and possible depletion of some heavy elements onto dust grains in Sect 6. Section 7 contains a brief discussion on the properties and nature of Mg II absorbing clouds.

2. Observations

2.1. Observations and data reduction

The observations were carried out at the F/8 Cassegrain focus of the 3.6 m telescope at La Silla, ESO Chile. The spectra were obtained with the ESO echelle spectrograph (CASPEC). A 300 line mm^{-1} cross disperser was combined with a 31.6 line mm^{-1} echelle grating for all objects, but Q2145 + 067 observed with a 52 line mm^{-1} echelle grating. The detector was a RCA CCD with 320 × 512 pixels of 30 μm square and a read-out noise of 45 electrons rms. Except for the brighter objects, the CCD was read-out binned in the direction of the dispersion with an effective pixel size of 60 × 30 $\mu\mathrm{m}^2$ to decrease the readout noise relative to the signal. For each exposure on the object a flat-field image and a wavelength comparison thorium spectrum were recorded. The slit width was of 2.″0 giving a resolution of FWHM = 1.9 px. The accuracy in the wavelength calibration has been measured on the calibrated throrium spectra. It is of 0.04 Å for the unbinned spectra, that is about one tenth of the resolution. The journal of the observations is shown in Table 1, which includes three high redshift quasars for which only the Mg II results are given in this paper. The detailed analysis of these high redshift quasars will be published in a forthcoming paper. Observations of Q2128-123 with the Image Photon Counting System of the University College London on the ESO 3.6 m telescope are also included in Table 1.

Table 1. Journal of observations

Object	Date year	day	Integration time (min)	Wavelength range (Å)	Resolution FWHM (Å)
0232–042	1986	285	100 + 100	4900 – 5950	0.65
0302–223	1986	283	75 + 75	4908 – 5950	0.65
0420–388	1985	205	90	5311 – 6426	0.65
	1985	206	120	5286 – 6385	0.65
0454+039	1986	284	80	4750 – 5800	0.65
1101–264	1986	013	120	4318 – 5375	0.37
	1986	014	100	5310 – 6427	0.37
2126–158	1984	155	90 + 90	4540 – 5731	0.65
	1985	206	90	5577 – 6734	0.65
2128–123	1981	164	100	3468 – 4450	0.95
	1985	284	60 + 60	5260 – 6320	0.37
2145+067	1984	236	90 + 90	4389 – 5510	0.55
2302+029	1986	284	75 + 75	4736 – 5805	0.65
2326–477	1985	285	90 + 90	5578 – 6690	0.65

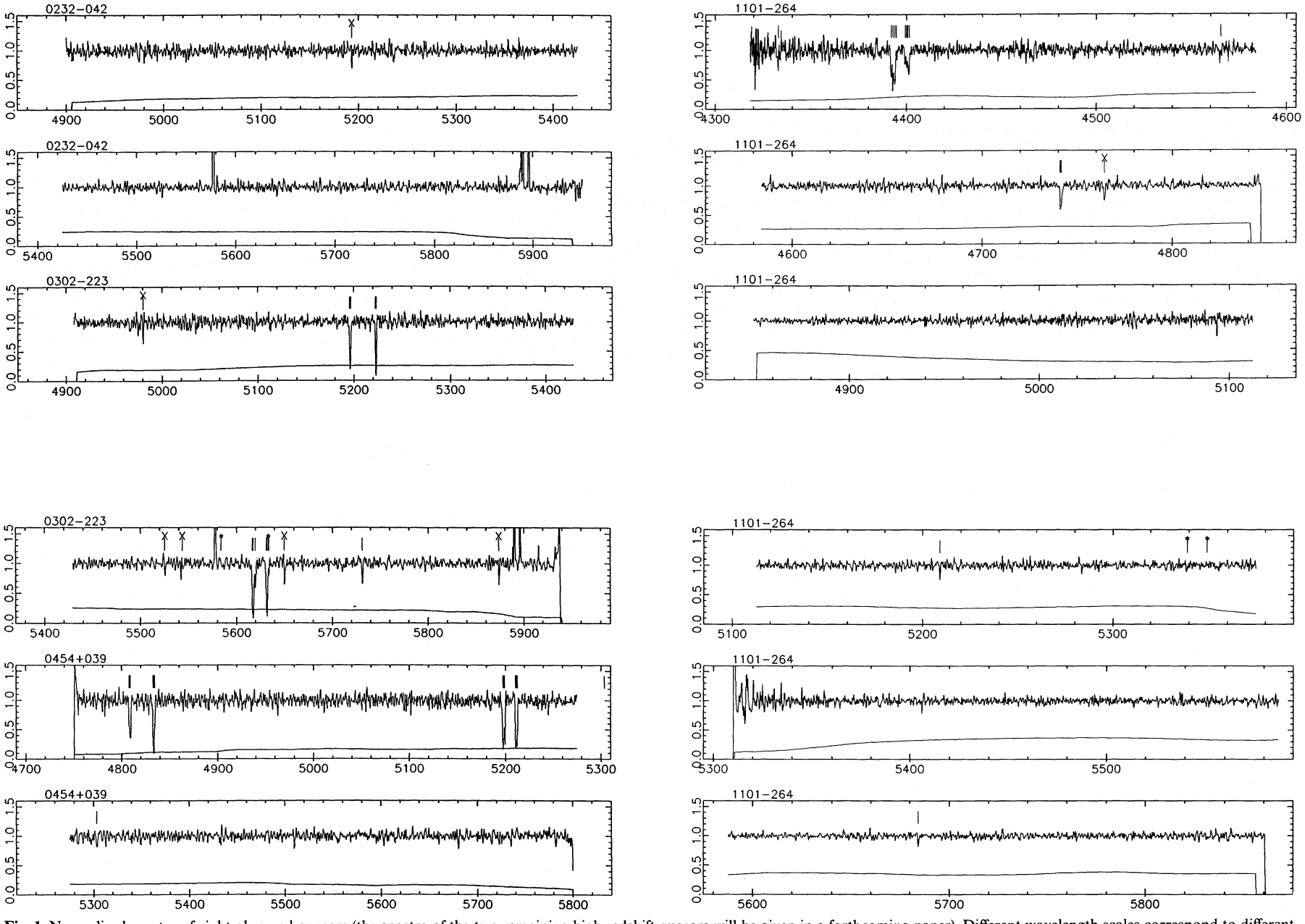

Fig. 1. Normalized spectra of eight observed quasars (the spectra of the two remaining high redshift quasars will be given in a forthcoming paper). Different wavelength scales correspond to different spectral resolutions such as the number of pixels be the same in each plot. The curve below the spectrum indicates the S/N ratio divided by 50. The features listed in Table 2 are marked by a straight line. Bad pixels are indicated by the sign X. Expected position for Ca II lines from previously known Mg II systems are marked by a star (★)

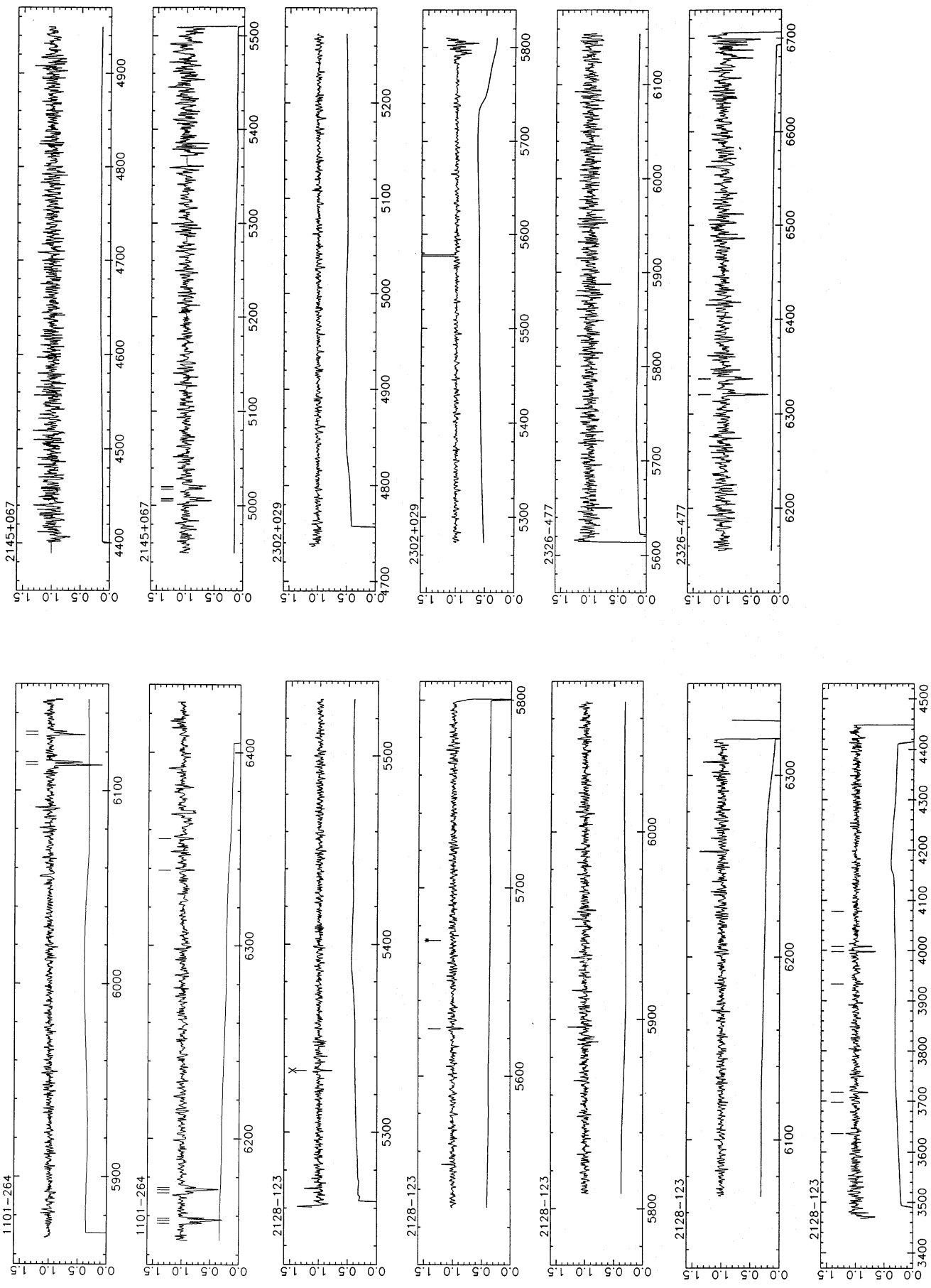

Fig. 1 (continued)

The data were reduced with the echelle reduction package implemented within MIDAS, the image processing system developed at ESO for Vax computers. The various steps of the data reduction have been described by D'Odorico et al. (1985). The results are presented in Fig. 1 (except for the high redshift quasars Q0420-388 and Q2126-158).

2.2. *Absorption lines*

To extract an homogeneous sample of absorption lines, we have computed the signal to noise ratio S/N for each spectrum. The continuum level has been determined by convolving the data with a Gaussian filter of $\sigma = 200$ px. Since the read-out noise dominates over the photon noise in our data, we have computed the S/N ratio by a maximum likelihood algorithm. The S/N ratio is given in Fig. 1 together with the spectra of the objects. It has been divided by 50 to have the same scale than the spectra. From this S/N ratio we have estimated the 4σ detection limit as a function of wavelength and the absorption lines detected at the 4σ level are given in Table 2.

When the observed line profile could not be fitted by a single component, we have used a line synthesis programme developed by D. Pelat (Pelat and Alloin, 1980) to derive the velocity dispersion and optical depth of each component of the blend. The oscillator strengths were taken from Morton et al. (1988).

2.3. *Notes on individual objects*

2.3.1. PKS 0232-042 $z_{em} = 1.434$

We do not detect any absorption line in the range $\lambda\lambda$ 4900-5950. There is no line either detected in a spectrum taken by Sargent

Table 2. Absorption lines

λ^a (Å)	W_{obs} (Å)	σ (Å)	Identification	z
		0232–042		
none				
		0302–223		
5197.01	1.15	0.05	FeII λ2586	1.00917
5197.59			FeII λ2586	1.00940
5224.20	1.26	0.05	FeII λ2600	1.00917
5224.79			FeII λ2600	1.00940
5618.07	1.78	0.06	MgIIλ2796	1.00907
5618.93			MgIIλ2796	1.00938
5621.24	0.56	0.06	MgIIλ2796	1.01021
5632.82	1.73	0.06	MgIIλ2803	1.00919
5633.33			MgIIλ2803	1.00937
5635.51	0.19	0.06	MgIIλ2803	1.01015
5732.86	0.36	0.06	MgI λ2852	1.00943
		0454 + 039		
4809.24			FeII λ2586	0.85926
4809.94	1.37	0.11	FeII λ2586	0.85953
4810.57			FeII λ2586	0.85977
4834.49			FeII λ2600	0.85929
4835.12	1.95	0.11	FeII λ2600	0.85953
4835.75			FeII λ2600	0.85977
5198.88			MgIIλ2796	0.85920
5200.02	2.02	0.08	MgIIλ2796	0.85957
5200.73			MgIIλ2796	0.85982
5212.33			MgIIλ2803	0.85920
5213.33	1.92	0.08	MgIIλ2803	0.85955
5213.97			MgIIλ2803	0.85978
5305.11	0.30	0.08	MgI λ2852	0.85950
		1101–264		
4334.20	0.12 :	0.03	SiII λ1526	1.83889
4393.41			CIV λ1548	1.83775
4394.23	1.28	0.03	CIV λ1548	1.83828
4394.80			CIV λ1548	1.83865
4395.33			CIV λ1548	1.83899
4400.71			CIV λ1550.	1.83776
4401.57	0.66	0.03	CIV λ1550	1.83831
4402.09			CIV λ1550	1.83865
4402.71			CIV λ1550	1.83905
4566.36	0.09 :	0.03	FeII λ1608	1.83897
4742.67	0.42	0.02	AlIIλ1670	1.83855
4743.20			AlIIλ1670	1.83886
5210.89	0.12	0.03	FeII λ2382	1.18691
5686.28	0.09	0.02	FeII λ2600	1.18688

Table 2 (continued)

λ^a (Å)	w_{obs} (Å)	σ (Å)	Identification	z
		1101–264		
6115.25	0.68	0.02	MgIIλ2796	1.18691
6116.78	0.44	0.02	MgIIλ2796	1.18746
6130.94	0.44	0.02	MgIIλ2803	1.18691
6132.49	0.18	0.02	MgIIλ2803	1.18746
6158.29	0.28	0.02	MgIIλ2796	1.20231
6159.76	0.72	0.02	MgIIλ2796	1.20284
6160.88	0.20	0.02	MgIIλ2796	1.20324
6173.96	0.19	0.02	MgIIλ2803	1.20226
6175.58	0.55	0.02	MgIIλ2803	1.20284
6176.72	0.21	0.02	MgIIλ2803	1.20324
6341.36	0.11	0.03	MgIIλ2796	1.26773
6357.54	0.13	0.03	MgIIλ2803	1.26769
		2128–123		
3718.20	0.38	0.07	FeII λ2600	0.42998
3934.37	0.17	0.07	CaII λ3934	-0.00010
3998.28	0.58	0.07	MgIIλ2796	0.42982
4008.74	0.53	0.07	MgIIλ2803	0.42989
4079.34	0.15	0.06	MgI λ2852	0.42986
5626.21	0.14	0.02	CaII λ3934	0.42987
		2145+067		
5006.31	0.47	0.08	MgIIλ2796	0.79030
5007.97	0.20	0.08	MgIIλ2796	0.79089
5009.10	0.35	0.08	MgIIλ2796	0.79130
5018.79	0.38	0.08	MgIIλ2803	0.79017
5020.87	0.32	0.08	MgIIλ2803	0.79087
5022.08	0.35	0.08	MgIIλ2803	0.79127
		2302+029		
none				
		2326-477		
6321.57	1.13	0.09	MgIIλ2796	1.26065
6322.23			MgIIλ2796	1.26089
6337.86	0.85	0.09	MgIIλ2803	1.26067
6338.56			MgIIλ2803	1.26092

[a] heliocentric vacuum values

et al. (1988a) at a resolution FWHM = 1.5 Å in the range λλ4040-5240.

2.3.2. PKS 0302-223 $z_{em} = 1.409$

Two Mg II absorption systems have been previously identified in this quasar at $z = 0.4196$ and 1.0095 (Bergeron, unpublished).

$z = 0.4196$: in our wavelength range we expect the Ca II doublet from this system for which we only obtain a 3 σ upper limit, w_{obs}(Ca II λ3934 or λ3969) < 0.16 Å.

$z = 1.0095$: the strong Mg II doublet is resolved in 3 components spanning 170 km s^{-1}. Two components have an associated strong Fe II λ2600 absorption. There is no Mn λ2576 absorption in any of the 3 subsystems at a 3 σ detection limit of $w_{obs} = 0.16$ Å.

2.3.3. PKS 0420-388 $z_{em} = 3.12$

There is no Mg II absorption doublet detected in the observed wavelength range λλ 5311-6385 and the average 1 σ level is 0.05 Å.

2.3.4. PKS 0454 + 039 $z_{em} = 1.345$

$z = 0.8595$: the Mg II absorption doublet breaks up into 3 components spanning 100 km s^{-1}. The Fe II λλ 2586,2600 doublet is strong for these 3 components. The Mg I λ2852 absorption is weak and the Mn II λ2576 is not detected at a 3 σ limit of $w_{obs} = 0.20$ Å.

2.3.5. Q 1101-264 $z_{em} = 2.148$

$z = 0.3564, 0.35903, 0.35923$: these systems have been detected in the Lyα forest of this quasar by Carswell et al. (1984). There is no associated Ca II absorption at a 3σ detection limit of $w_{obs} = 0.05$ Å, which confirms the 3 σ non detection of 0.06 Å reported by Robertson et al. (1988).

$z = 1.1875$: the Mg II system found at low resolution by Boissé and Bergeron (1985) is a blend of two components separated by 75 km s^{-1}. There is an associated Fe II absorption for only one component and no detection of Mn λ2576 and Mn I λ2852 at a level of $w_{obs} = 0.05$ and 0.08 Å respectively.

$z = 1.2030$: this system was also detected by Boissé and Bergeron (1985) and is triple with components spread over 130 km s^{-1}. There is no other line detected for this system and limits for the Mn λ 2576-Fe II λ 2600 range and Mg I λ 2852 are the same than for the $z = 1.1875$ system.

$z = 1.2677$: this Mg II system is the weakest of our sample, although the Mg II doublet is saturated. Both lines are detected at the 4 σ level.

$z = 1.8387$: we find as Carswell et al. (1984), that the C IV complex is quadruple and our redshift estimate for the 4 components is consistent with their within the observational uncertainty. There is associated Al II λ 1670 and Fe II λ 1608 absorption for two and one components respectively. The Si II λ 1526 absorption falls at the edge of our spectrum and its equivalent width is highly uncertain.

2.3.6. PKS 2126-158 $z_{em} = 3.275$

There is no Mg II absorption doublet detected in the observed wavelength range $\lambda\lambda$ 4540-6734 and the average 1 σ level is 0.04 Å.

2.3.7. PKS 2128-123 $z_{em} = 0.501$

$z = 0.4299$: this system has been discovered in one of the first Mg II survey by Weymann et al. (1979) and the associated absorbing galaxy has been identified by Bergeron (1986). There is an associated Ca II K absorption and the Ca II H could be present at the 1 σ level. We also give for this quasar a spectrum covering the Fe II and Mg II absorption ranges, taken at a resolution of FWHM = 0.95 Å, which is of higher S/N ratio, especially for the Fe II lines, than that obtained by Tytler et al. (1987). The Fe II λ 2586 line is present at the 2 σ level with $w_r = 0.14$ Å, at $\lambda_{helio} = 3699.05$ Å.

The weak resolved (FWHM$_{obs}$ = 2.9 Å) emission line with $w_{obs} = 0.67$ Å, at $\lambda_{helio} = 3637.01$ Å, is identified with [Ne IV] $\lambda\lambda$ 2421,2424 doublet at $z = 0.5012$.

2.3.8. PKS 2145 + 067 $z_{em} = 0.990$

$z = 0.791$: the Mg II doublet observed at 1.5 Å resolution by Sargent et al. (1988a) is the blend of 3 components spanning 170 km s^{-1}. There is no detection of Mn II λ 2576, Fe II λ 2600 and Mg I λ 2852 at a 3 σ level of $w_{obs} = 0.18$, 0.21 and 0.27 Å respectively.

2.3.9. PG 2302 + 029 $z_{em} = 1.044$

No line is detected over the range $\lambda\lambda$ 4736-5805 for this bright radio-quiet quasar. The average 1 σ level is 0.02 Å.

2.3.10. PKS 2326-477 $z_{em} = 1.306$

$z = 1.261$: strong C IV and weak Mg II absorptions have been previously discovered in this quasar at 5910 km s^{-1} from the emission redshift (Bergeron, unpublished). The Mg II lines are a blend of two components separated by 60 km s^{-1}. There is no associated Mn II λ 2576, Fe II λ 2600 and Mg I λ 2852 absorption at a 3 σ level of $w_{obs} = 0.18$, 0.18 and 0.15 Å respectively. There is a possible 3σ absorption at $\lambda = 6338.75$ Å.

3. Weak Mg II systems: evolution in redshift

As mentioned in Sect. 1, the difference in the cosmological evolutions of the number density of Mg II and Lyman limit systems may vary with the equivalent width limit of the Mg II samples considered. This would be a consequence of the evolution with redshift of the fraction of weak to strong Mg II systems, thus of the evolution of the low w_r end of the Mg II equivalent width distribution. We have found such an evolution by analysis of Mg II samples at different redshifts and we also have tested this assumption on our own data.

The samples we have considered are in order of increasing average redshift those of Boulade et al. (1987), M25 of Tytler et al. (1987), MG1 of Sargent et al (1988a) and M1 of Lanzetta et al. (1987). The rest equivalent width limits of these surveys are no larger than $w_{r,min} = 0.3$ Å and altogether there are 19, 22 and 16 systems in the redshift ranges 0.11–0.5, 0.5–1.0 and 1.0–2.1 respectively. For these redshift intervals, the number R of systems with w_r(Mg II λ 2796) $\geq$ 0.3 Å relative to those with w_r(Mg II λ 2796) $\geq$ 0.6 Å equals 3.2, 2.0 and 1.3 respectively. If only the MG1 sample of Sargent et al. (1988a) is considered, a similar trend remains with values of R equal to 3.0, 2.1 and 1.8 in the redshift bins 0.2–0.5, 0.5–1.0 and 1.0–1.5 respectively and a total number of systems in each bin of 9, 17 and 11. These values of R can be compared with the ratio R_{LLS} of Lyman limit systems to Mg II systems with w_r(Mg II λ 2796) $\geq$ 0.6 Å. The number density of LLS as a function of z is taken from Lanzetta (1988). The dependence in redshift is $(1 + z)^{\gamma}$ with $\gamma = 0.48 \pm 0.44$, which is roughly consistent with no evolution for $q_0 = 0$ or 1/2. For Mg II systems with $w_r \geq 0.6$ Å, we use the number density at $z = 0.51$ given by Tytler et al. (1987) and the cosmological evolution estimated by Boulade et al. (1987), $\gamma = 2.0 \pm 0.5$. For the above redshift ranges of 0.11–0.5, 0.5–1.0 and 1.0–2.1, we find values of R_{LLS} of 5.3, 3.4, 1.9.

These results strongly suggest that Mg II samples with decreasing $w_{r,min}$ should show less and less evolution. We have estimated the redshift dependence of the $w_{r,min} = 0.3$ Å composite sample described above using that of the $w_{r,min} = 0.6$ Å Mg II sample and applying the correction factor R. We find $\gamma(w_{r,min} = 0.3$ Å$) \sim 0.7$ which implies very little cosmological evolution. We have obtained very similar results for R_{LLS} and $\gamma(w_{r,min} = 0.3$ Å) using the data from the LLS survey of Sargent et al. (1989). Caulet (1989) has reached similar conclusions, using her own Mg II survey and extrapolating to $w_r = 0.15$ Å the equivalent width distributions of Lanzetta et al. (1987) and of Tytler et al. (1987). She found values of $\gamma = 1.95$, 1.04 and -0.05 for $w_{r,min} =$ 0.6, 0.3 and 0.15 Å respectively.

The increase in the fraction of weak to strong Mg II systems with decreasing redshift may appear inconsistent with the lack of correlation between the Mg II equivalent width distribution and z found by Lanzetta et al. (1987) and Sargent et al. (1988a). However, their results essentially concern the bulk of the w_r distribution rather than the behaviour at small w_r. Tytler et al. (1987) have fitted the Mg II equivalent width distribution by a power law $n(w_r) \propto w_r^{-\delta}$ with $\delta = 2.1 \pm 0.3$ at an average redshift $\bar{z} = 0.51$ for systems with w_r(Mg II λ 2796) $\geq$ 0.25 Å. Combining their lower redshift survey ($\bar{z} = 0.23$) to that of Tytler et al. (1987), Boulade et al. (1987) give $\delta = 2.2 \pm 0.2$. For higher redshift samples, exponential forms have been considered and within the uncertainties similar fits are obtained at $\bar{z} = 0.73$ (Sargent et al. 1988a) and $\bar{z} = 1.62$ (Lanzetta et al., 1987). However for the intermediate redshift sample there are more weak Mg II doublets than predicted by the assumed exponential distribution, whereas at higher redshift the fit is also satisfactory for the weaker systems. For the $\bar{z} = 0.73$ sample we have found that a better fit is obtained with a power law of index $\delta \sim 1.6$. This could be interpreted as evidence for a turn-over in the w_r distribution between $w_r = 0.3$

and 0.6 Å for Mg II systems at $\bar{z} = 1.6$, whereas a turn-over could occur only at $w_r < 0.3$ Å for $\bar{z} = 0.7$ samples.

A large number of known Mg II systems was included a priori in our sample for kinematical studies discussed in the following sections. However our sample remains unbiased for Mg II doublets with small equivalent widths. The average redshift of our survey is close to unity. For the sample with $w_{r,\min}(\text{Mg II}\,\lambda 2796) = 0.15$ Å, it is equal to $\bar{z} = 0.98$ (see Table 3, next section). There is only one new system detected with $w_r(\text{Mg II}\,\lambda 2796) \sim w_r(\text{Mg II}\,\lambda 2803) \sim 0.05$ Å at $z = 1.2677$ towards Q1101-264 (see Table 2). To investigate further this paucity of weak ($w_r(\text{Mg II}\,\lambda 2796) < 0.3$ Å) Mg II systems in our sample we have constructed the auto-correlation function restricted to data in spectral windows satisfying $w_{r,\min} \leq 0.25$ Å. We have carefully removed absorption lines from known redshift systems and have smoothed the remaining spectra to obtain the continuum level. We have derived the auto-correlation function for each spectrum and co-added the results for all spectra. If weak Mg II doublets were present we should have a peak at the separation of the Mg II doublet, but no signal is detected at the 3σ level.

To test further the possible evolution of the low end of the Mg II w_r distribution, we have estimated the predicted number of weak Mg II systems, based on an assumed power law distribution of Mg II equivalent widths as found at $\bar{z} = 0.5$ (Tytler et al., 1987) and compare it to our observations. The distribution has been normalized using the number density per unit redshift of the M25 sample of Tytler et al. (1987) corrected for a cosmological evolution $\gamma = 2.0$ (Boulade et al., 1987) at the average redshift of our samples $\bar{z} \sim 1$. For each quasar spectrum we give in Table 3 the redshift windows in which we can detect absorption lines at the 4σ level with $w_{r,\min} = 0.3$, 0.15 and 0.05 Å. The corresponding samples are labelled S30, S15 and S5 respectively. Since our observations are biased towards strong Mg II doublets we have estimated the expected number of Mg II systems only up to $w_r(\text{Mg II}\lambda 2796) = 0.5$ Å, which we give in Table 3 together with the number of detected systems. There is a large discrepancy between the expected and detected numbers of Mg II doublets for the S15 and S5 samples: 4.5 and 5.5 are expected respectively whereas 0 and 1 are found. Taking a weaker cosmological evolution, $\gamma = 1.0$, would not drastically modify this conclusion since the expected number of Mg II systems would only be smaller by a factor of 1.35 than the values quoted above. These results not only strengthen the assumption of an evolution of the low w_r end of the Mg II w_r distribution but also clearly suggest that at $z \sim 1$ there is a strong break in this distribution at $w_r < 0.3$Å.

At $z \sim 2$, LLS are of low or mixed ionization level with singly ionized elements (C II, Mg II, Si II or Fe II) always present. The diffuse UV background is the most likely ionization source of the absorbers (see e.g. Sargent et al., 1980; Bergeron and Stasińka, 1986), and the number of ionizing photons is roughly evolving as $(1+z)^4$ for $z \leq 2$. Thus at $z \sim 0.5$–1.0, LLS should also show Mg II absorption since the ionization level of the absorbers should be lower than at $z = 2$. We can derive an upper limit of the break in the w_r distribution of Mg II systems assuming that all Mg II systems are LLS and a power-law distribution with a sharp cut-off. This is only an upper limit not only because the turn-over could be gradual but mainly because at low z some Mg II systems could be optically thin (Bergeron and Stasińska, 1986). Using the same assumptions than above for LLS and the M25 Mg II sample of Tytler et al., (1987), we find upper limits for Mg II distribution cut-off of 0.16, 0.24 and 0.41 Å for $z = 0.5$, 1.0 and 2.0 respectively. This is consistent with the paucity of weak Mg II systems found in the present survey, and with the w_r distributions of Mg II systems given by Tytler et al. (1987), Lanzetta et al. (1987) and Sargent et al. (1988a). Further our results suggest that at $z \sim 1$, the number of optically thin Mg II systems is much smaller than would be derived assuming a single power law distribution for all Mg II systems extending to very small w_r(~ 0.05 Å as for the weak system detected towards Q1101–264).

Table 3. Mg II absorption systems: redshift windows and samples

Quasar	z_e	<S/N>	S30[a]		S15		S5	
			z_{min}	z_{max}	z_{min}	z_{max}	z_{min}	z_{max}
0215+015	1.649	28	1.017	1.398	1.017	1.398	1.056	1.387
0232–042	1.434	11	0.752	1.127	0.806	1.076		
0302–223	1.400	12	0.752	1.127	0.806	1.069		
0420–338	3.12	9	0.899	1.251	0.970	1.10		
0454+039	1.354	8	0.752	1.033				
1101–264	2.148	15	0.552	0.919	0.552	0.919		
		17	0.919	1.269	0.919	1.269	0.935	1.211
1327–206	1.165	10	0.859	1.104	0.859	1.051		
2126–158	3.275	12	0.88	1.003	0.880	1.015		
		12	1.003	1.39	1.003	1.354		
2145+067	1.000	8	0.627	0.873	0.699	0.855		
2302+029	1.044	27	0.694	1.000	0.694	1.000	0.913	1.051
2326–477	1.299	8	1.020	1.25				
$\Sigma\Delta z$			4.02		2.91		0.75	
$\bar{z}$			0.99		0.98		1.11	
Nexpected			1.7		4.5		5.5	
Ndetected			0		0		1	

[a] the redshift windows for a S25 sample are indentical to those of S30

Table 4. Model fit parameters for the subcomponents

subcomponent number	z	Δv (km s^{-1})	Mg I		MgII		FeII		MnII	
			N (10^{12}cm^{-2})	b (km s^{-1})	N (10^{12}cm^{-2})	b (km s^{-1})	N (10^{12}cm^{-2})	b (km s^{-1})	N (10^{12}cm^{-2})	b (km s^{-1})
					0215 + 015[d]					
1	1.34375	0	0.84	17.1	53.	14.5	20.	17.1	< 2.	
2	1.34407	41	0.32	15.	19.	10.1	22.	9.4	< 2.	
3	1.34468	119	0.63	21.5	45.	17.8	84.	26.5	2.1	7.8
4	1.34513	177	1.00	37.6	190.	30.1	64.	25.2	1.0	10.2
					0302 − 223					
1	1.00931	0	< 0.23		12.	16.3	31.	6.7	< 1.8	
2	1.00962	46	2.5	16.4	65.	29.5	166.	15.9	< 1.8	
3	1.01045	170	< 0.23		9.7	13.2	< 2.9		< 1.8	
					0454 + 039					
1	0.85927	0	< 0.49		41.	28.4	66.	28.4	< 2.2	
2	0.85964	60	0.69	13.1	17.	14.7	75.	14.7	< 2.2	
3	0.85989	100	< 0.49		21.	19.	117.	19.	< 2.2	
					0735 + 078[e]					
1	0.42330	0			25.	18.				
2	0.42361	65	1.3		15.	18.				
3	0.42382	109			20.	17.				
4	0.42409	165			9.	12.				
					1101 − 264					
1	0.35635[g]	0			6.3	11.				
1(2)	0.35903[g]	0(593)			24.	9.	> 8.	< 15.		
2(3)	0.35923[g]	43(636)			12.	14.	> 2.5	< 26.		
1	1.18691	0	< 0.29		13.[a], 7.5	16.[a], 8.6	3.4[b]		< 2.1	
2	1.18746	75	< 0.29		7.	15.	< 1.5		< 2.1	
1	1.20231	0[c]	< 0.29		5.8[a], 5.	6.7[a], 19.	< 1.5		< 2.1	
2	1.20284	72	< 0.29		47.[a], 27.	13.[a], 19.	< 2.2		< 2.1	
3	1.20324	127	< 0.29		2.2[b], 2.5	< 6.5	< 1.5		< 2.1	
1	1.26773	0			1.2[b]					
					1327 − 206[f]					
1	0.84983	0	< 0.31		7.7[a], 6.	8.[a], < 15.				
2	0.85032	79	0.54	< 15.	26.[a], 18.	13.[a], < 15.				
3	0.85136	248	0.29	< 15.	8.5	< 15.				
4	0.85197	347	< 0.31		19.[a], 9.2	10.[a], 31.				
5	0.85269	464	< 0.31		18.[a], 20.	24.[a], 17.	{ 52.			
6	0.85327	558	0.83	< 15.	48.[a], 42.	28.[a], 36.	{			
					2128 − 123					
1	0.42990	0	1.7	8.	139.	8.6	187.	8.6		
					2145 + 067					
1	0.79057	0	< 0.44		4.9	< 15.	< 4.		< 2.	
2	0.79116	99	< 0.44		5.0	< 15.	< 4.		< 2.	
3	0.79157	167	< 0.44		6.5	< 15.	< 4.		< 2.	
					2326 − 477					
1	1.26098	0	< 0.35		9.	< 10.	< 5.5		< 3.9	
2	1.26122	57	< 0.35		7.3	< 10.	< 5.5		< 3.9	

[a] Doublet ratio method.
[b] Optically thin case. Further all the upper limits are calculated in the optically thin case.
[c] The velocity separation of this component and the one at z_{abs}=1.18691 is 2105 km s^{-1}.
References : [d] Bergeron and D'Odorico (1986), [e] Boksenberg et al. (1979), [f] Bergeron et al. (1987, with values given in this paper corrected from a misprint), [g] Carswell et al. (1984)

We now want to stress that the evolution in the number of weak Mg II systems with redshift may be understood in two ways. It could represent a true evolution of the size of Mg II halos down to a given Mg II column density. Such a situation may arise if the outer parts of gaseous halos, of smaller density than the inner regions, have an ionization level decreasing with decreasing z. This would imply that the increase in equivalent width reflects an increase in column density. However, the sequence in equivalent width is probably a sequence in line multiplicity as suggested by Wolfe (1986) and discussed in this paper (Sect. 4 and 5). The evolution in the Mg II w_r distribution could then be an evolution in the average number of clouds in galactic halos per line of sight, due to an evolution either in the gas distribution and/or its velocity field.

4. Clustering of Mg II clouds

Clustering of metal-line systems has already been extensively investigated for C IV samples (Young et al., 1982; Sargent et al., 1988b). The two-point correlation function for the C IV redshifts is flat on scales above 2000 km s^{-1} and shows a significant excess at velocity separations up to 600 km s^{-1}. This is interpreted to reflect galaxy-galaxy clustering. If kinematics of interstellar gas are not strongly evolving with redshift, relative motions of individual clouds within galaxies are unlikely to account for these large C IV velocity separations (Sargent et al., 1988b); however they could explain the clustering found on a scale $\Delta v \leq 200$ km s^{-1} in the Mg II sample of Sargent et al. (1988a). The small size of published Mg II samples casts some doubts on the presence of only cloud-cloud clustering, since the rareness of Mg II velocity separations beyond 200 km s^{-1} prevents detection of clustering on scales $200 \leq \Delta v \leq 600$ km s^{-1} at the level found for C IV redshifts.

To increase our sample, which is at higher spectral resolution than those previously published, we have included earlier observations at similar resolution than our own, namely those of Q0215 + 015 (Bergeron and D'Odorico, 1986), Q0735 + 178 (Boksenberg et al., 1979), Q1101-264 (Carswell et al., 1984) and Q1327–206 (Bergeron et al., 1987). The overall Mg II sample is represented in Table 4. The system at $z = 0.35635$ in Q1101–264 (Carswell et al., 1984) is double with a velocity separation of 24 km s^{-1} but has been considered as single in our velocity analysis, to have an homogeneous sample on velocity scales $\Delta v \geq 30$ km s^{-1}.

4.1. *Two-point correlation function*

Following Sargent et al. (1980), we have estimated the comoving separations between all subcomponents and derived the two-point correlation function for the Mg II clouds. Results are shown in Fig. 2 with 50 km s^{-1} bins. The calculations have been made assuming $q_0 = 1/2$. There is adequate information on scales up to 700 km s^{-1}. At higher velocity separations, there are too few systems for any meaningful analysis. We note that in Fig. 2 the local peak at $\Delta v \sim 2000$ km s^{-1} is due to two multiple systems on a single line of sight (Q1101-264).

To better analyze the possible contributions of either cloud-cloud or galaxy-galaxy clustering to the two-point correlation function, we have tried to fit the distribution of observed velocity separations with a single Gaussian. We have restricted the fit to scales $30 \leq \Delta v \leq 700$ km s^{-1}. Further to minimize the uncertainty on individual values of the Δv distribution we have used bins of different size, with a minimum width of 20 km s^{-1}, containing each at least 5 pairs. There are 43 pairs in the velocity interval considered. The overall distribution is normalized to obtain a probability of unity for finding a velocity separation in the range 30–700 km s^{-1}. The results are plotted in Fig. 3. A single Gaussian gives a poor fit. The χ^2 value is 18.8 and, for six degrees of freedom, has the probability 0.01 to be overtaken. This reflects the clear excess of velocity separations beyond 400 km s^{-1}. The maximum deviation between the observed and

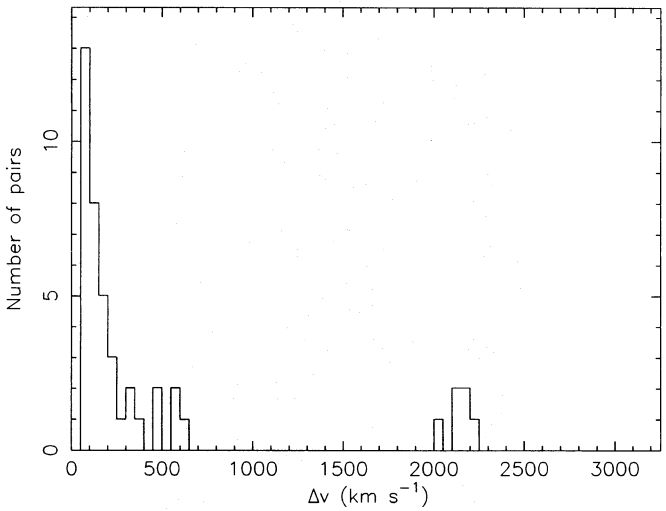

Fig. 2. Two point correlation function for the Mg II systems in the sample described in Table 4. The number of line pairs is plotted against the velocity separation Δv between subcomponents. The mean level for a Poisson distribution is not indicated because of the lack of observation for $\Delta v > 700$ km s^{-1}

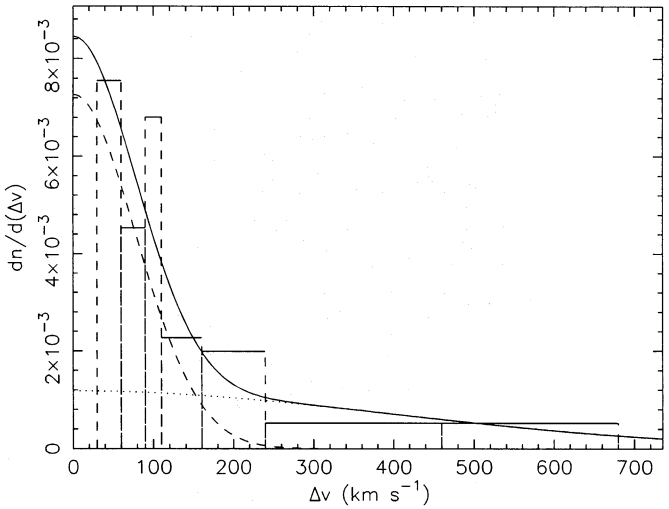

Fig. 3. Distribution of the velocity separation Δv between subcomponents, normalized for Δv in the range 30–700 km s^{-1}. The data are binned so that there are at least 5 points per bin. The solid line is the best fit to the data using a sum of two Gaussian distributions with $\sigma_v = 390$ km s^{-1} (dotted line) and $\sigma_v = 80$ km s^{-1} (dashed line). The quality of the fit can be appreciated in Fig. 4

modeled cumulative distributions in the Kolmogorov-Smirnov test is 0.1, and has the probability 0.40 to be overtaken.

We have then used a two-component model of the form

$$f(\Delta v) = \sqrt{\frac{2}{\pi}}\left(\frac{A}{\sigma_a}\exp\left(-\frac{\Delta v^2}{2\sigma_a^2}\right) + \frac{1-A}{\sigma_b}\exp\left(-\frac{\Delta v^2}{2\sigma_b^2}\right)\right), \quad (1)$$

and the probability to find two subcomponents separated by Δv_0 in the range 30–700 km s^{-1} is

$$p(\Delta v_0) = \frac{f(\Delta v_0)d(\Delta v)}{\int_{30}^{700} f(\Delta v)d(\Delta v)} \quad (2)$$

The best fit and the individual Gaussians are plotted in Fig. 3. The χ^2 value is 0.07 and, for six degrees of freedom, has the probability 0.95 to be overtaken. The Kolmogorov-Smirnov test on the cumulative distribution is 0.06 and has the probability 0.74 to be overtaken. The observed and modeled cumulative distributions are shown in Fig. 4. The two components have similar weight, $A = 0.55$, and the rms dispersions are $\sigma_a = 80\,\mathrm{km\,s^{-1}}$ and $\sigma_b = 390\,\mathrm{km\,s^{-1}}$.

The Δv distribution of the broader component may be compared with those obtained for correlated galaxy pairs outside rich clusters and for galaxies in clusters. Davis and Peebles (1983) and De Lapparent et al. (1988) have derived the dispersion of the distribution of relative velocity between galaxy pairs as a function of the pair linear separation. Values of σ similar to that derived for the broader component of the Mg II Δv distribution are observed for galaxy pairs with, however, a large projected linear separation of $3.0h^{-1}$ Mpc (h is the Hubble constant in units of 100 km s^{-1} Mpc^{-1}). Much larger values of σ are found for galaxies in clusters. For the Virgo cluster, Tully and Shaya (1984) give for the velocity distribution of early- and late-type spiral galaxies rms dispersions of 793 and 687 km s^{-1}, which yields for the velocity distribution between galaxies values larger by $\sqrt{2}$, i.e. of 1120 and 97 km s^{-1}. For 107 rich clusters the median of the galaxy velocity dispersion is 650 km s^{-1} and the same value is obtained if the sample is restricted to the 38 clusters containing a cD or D galaxy (Geller, 1987). This yields a dispersion of 920 km s^{-1} for the velocity distribution between galaxies.

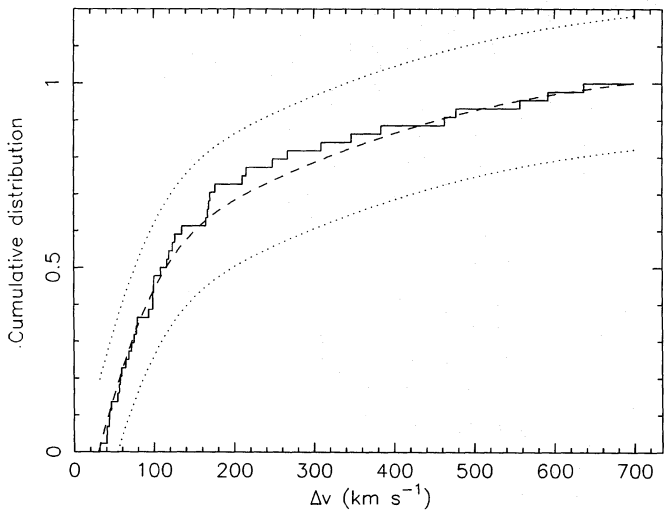

Fig. 4. The observed and fitted cumulative distributions of velocity separation Δv between subcomponents. The fit is the sum of the two Gaussian distributions plotted in Fig. 3. the dotted curves correspond to the 80% confidence level limits for the Kolmogorov test statistic

Accounting for Mg II line multiplicity by pairs of galaxies rather than galaxies in clusters is consistent with identification of Mg II absorbers which are usually found to be field galaxies (Bergeron, 1988a). Identification of a Mg II multiple system, spanning at least 400 km s^{-1}, by more than one absorbing galaxy should be made to confirm the assumption of galaxy pairs. Another possible explanation would be merging of galaxies with a highly disturbed velocity field. Spectroscopic observations of galaxy candidates close on the sky to Q1327-206 are unfortunately inconclusive, the objects being very faint (Bergeron, unpublished). The other case given in Table 4, Q1101-264, may favor the galaxy pair assumption since the galaxy at $z = 0.359$ has neither a disturbed morphology nor broad emission lines (FWHM < 600 km s^{-1}); however the absorber at $z = 0.356$ is still to be found (Bergeron and Boissé, 1989, in preparation).

4.2. *Kinematic model*

To test whether the two component model, needed to reproduce the observed distribution of velocity separations, involves one or two distinct populations we have modelled the expected number of clouds per line of sight and their maximum velocity separation in the assumption of a collection of clouds belonging to a single population.

We consider a simple model assuming for all components of a given absorber, clouds of identical size, randomly distributed within either a sphere or a disk, and with a one or two component Gaussian velocity distribution. The sphere has a radius R and the disk is of infinite radius and height h. If l is the length of a line of sight within the absorber, the probability to have l compromised between l and $l + dl$ is

$$dp = \frac{l}{2R^2}dl \quad \text{for the spherical case,} \quad (3)$$

$$dp = \frac{h}{l^2}dl \quad \text{for the disk case.} \quad (4)$$

Assuming a Poissonian cloud distribution, the probability to find n clouds along l is $(\lambda l)^n\frac{e^{-\lambda l}}{n!}$ where λ is the mean number of clouds per unit distance. This gives for the probability to encounter n clouds on a line of sight passing through an absorber

$$p(n) = \int_0^{2R}\frac{(\lambda l)^n e^{-\lambda l}}{n!}\frac{l}{2R^2}dl = \frac{2}{\bar{n}^2}\int_0^{\bar{n}}\frac{u^{n+1}e^{-u}}{n!}du, \quad (5)$$

for the spherical case, where $\bar{n} = 2\lambda R$ and

$$p(n) = \int_h^{+\infty}\frac{(\lambda l)^n e^{-\lambda l}}{n!}\frac{h}{l^2}dl = \bar{n}\int_{\bar{n}}^{+\infty}\frac{u^{n-2}e^{-u}}{n!}du, \quad (6)$$

for the disk case, where $\bar{n} = \lambda h$.

For a given cloud velocity distribution, we have determined the velocity of individual clouds by random trials. We have considered as a single component all the clouds with a velocity separation smaller than our resolution, $\Delta v_{\min} = 30\,\mathrm{km\,s^{-1}}$, and have computed the probability $b(n_s, n)$ of detecting n_s subcomponents on a line of sight encountering n clouds. The probability to detect n_s subcomponents in any Mg II absorber is then

$$p(n_s) = \sum_{i=1}^{+\infty} p(i) \times b(n_s, i). \quad (7)$$

Table 5. Estimated and observed normalized distributions of Mg II components.

geometry	$\bar{n}$	σ_1	σ_2	n_s								$\bar{n}_{bl}$
		km s^{-1}		0	1	2	3	4	5	6	7	
				models								
disk	3	75		0.01	0.13	0.32	0.33	0.16	0.04	0.01	0.00	4.8[a]
sphere	5	100		0.08	0.19	0.29	0.25	0.14	0.04	0.01	0.00	1.3 ± 0.8
sphere	5.1	55	278	0.07	0.23	0.23	0.25	0.13	0.06	0.02	0.01	1.3 ± 0.7
				observations								
					0.23	0.23	0.31	0.15	0.00	0.08	0.00	

[a] the uncertainty is large but meaningless in the case of infinite radius

We have estimated this probability and derived the mean velocity separation of the subcomponents and the mean number of clouds blended in a subcomponent for the one and two component models of the velocity separation distribution given in Sect. 4.1.

The average number of clouds $\bar{n}$, and the rms dispersion σ of distribution(s) have been adjusted to fit the observed n_s distribution. The results are given in Table 5 together with the normalized observed distribution. We have assumed that the three components at $z \sim 0.36$ in Q1101-264 belong to two distincts absorbers with velocity separation of about 615 km s^{-1}. This choice is motivated by the identification of an absorbing galaxy 12″ away on the sky from the quasar, at a redshift $z = 0.359$, equal to that of the two absorption subcomponents of higher velocity (Bergeron and Boissé, 1989, in preparation).

The number of subcomponents detected per line of sight is roughly constant from n_s equal 1 to 3, and beyond it is smoothly decreasing. There is not a large difference between the spherical and disklike models, and our sample is too small to favor a particular geometry. For a single velocity distribution, the best fit is obtained for a somewhat larger value of the velocity dispersion in the spherical case than for the disk configuration; this is due in part to our assumption of a disk with infinite radius. A two component model gives a better fit than a single population. We give in Table 5 results for a spherical geometry, and the velocity dispersions which best reproduce the observed distribution of velocity separations (the values given in Sect. 4.1 have been divided by $\sqrt{2}$ for applying to a cloud velocity distribution). This model fits well the observed distribution of subcomponents. If the Mg II absorption systems in Q1101-264 at $z \sim 0.36$ had been considered to belong to a single absorber, the peak at $n_s = 3$ would have been much more pronounced (giving for n_s from 2 to 7 a normalized observed distribution of 0.17, 0.17, 0.41, 0.17, 0.00 and 0.08) resulting in a large discrepancy between the observations and the models. The mean number of clouds per subcomponent is much larger in the disk than in the spherical case and observations at very high spectral resolution may help to distinguish between the two geometries.

The maximum velocity separation between subcomponents Δv_m on a line of sight as a function of n_s can be derived from the models described above. Results are shown in Fig. 5 for the three models given in Table 5. A reasonable fit to the observations is obtained for a single velocity distribution but only for $n_s < 5$. A two velocity component model roughly accounts for all the cases but predicts in average larger values of Δv_m than observed for a number of subcomponents in the range 2 to 4. Assuming a single absorber for the triple system at $z \sim 0.36$ in Q1101-264 would give a point ($\Delta v_m = 636$ km s^{-1}) well outside the rms dispersion of Δv_m for all the models.

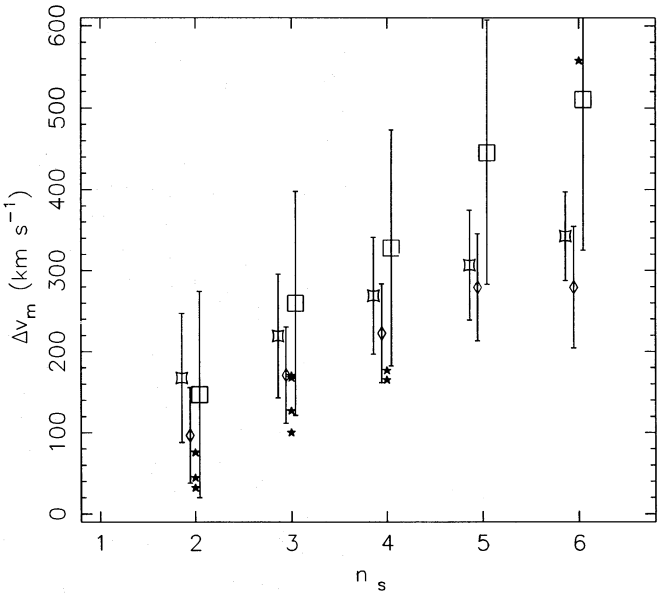

Fig. 5. The maximum velocity separation between subcomponents of a given absorber, Δv_m, versus the number of subcomponents for the Mg II sample given in Table 4. The observed points are labelled as stars (★). the expected values and rms are plotted for the models 1(⌻), 2(◇) and 3(□) described in Table 5

In conclusion, a single population model with two components of different velocity dispersions gives a good representation of the distribution of the number of observed Mg II subcomponents, except if the triple system mentioned above is considered as a single absorber. However the maximum velocity separation as a function of the number of subcomponents is not well fitted by either one or two velocity components within a single population, even more so if the triple system in Q1101-264 belongs to a single absorber. Therefore, our modelling of the number of Mg II subcomponents and their maximum velocity separation suggests that the two components, implied by the observed distribution of velocity separation between Mg II absorption subcomponents, refer to two distinct populations: clouds within galaxies and galaxy pairs.

5. Line equivalent width, multiplicity and column density

In the previous section, we have seen that the clustering of Mg II absorbing clouds is strongest at the lowest velocity separation observable at our spectral resolution (lowest Δv bin of 30–60 km s^{-1}). Absorption lines detected in moderate spectral resolution surveys will therefore usually be blends of subcomponents and the observed equivalent widths will be a function of the number of individual clouds and of their column densities.

The trend of increasing equivalent width with increasing multiplicity of the absorption systems has already been recognized (Wolfe, 1986; York et al., 1986). We have investigated whether this led to a well-defined correlation at our spectral resolution. Although we may not have reached the ultimate individual components, we have also searched for a correlation between equivalent widths and column densities for single entities as detected at our resolution.

There is a strong correlation between the total equivalent width of an absorber, $w_{r,\mathrm{tot}}$, and the subcomponent multiplicity, n_s, as shown in Fig. 6. The individual components are described in Table 4. At $\bar{z} \sim 1$, the total equivalent width scales linearly with the number of clouds and the best fit, plotted in Fig. 6, has a high correlation ratio of 0.91; this fit is close to a proportionality. If such a correlation holds whatever z, the paucity of weak Mg II systems in higher redshift samples would then imply that the $z \sim 1.5$–2 Mg II systems are almost always multiple.

To derive the column density and velocity dispersion b of individual components, we have used both the doublet ratio method and a line profile fitting method which assumes a Gaussian velocity dispersion for individual clouds. The results are given in Table 4. The b distribution, plotted in Fig. 7, shows a strong increase with decreasing values of b with a turn-over in the velocity bin at 5–10 km s^{-1}. This turn-over is due, at least in part, to an observational bias as only a small fraction of our observations have been made at a high enough spectral resolution. If the derived b distribution represents the true distribution

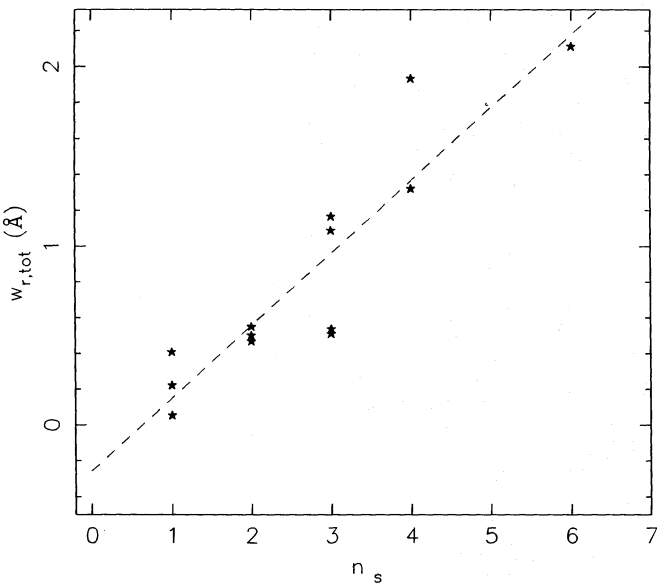

Fig. 6. Total rest equivalent width ($w_{r,\mathrm{tot}}$) of Mg II λ2796 for the systems given in Table 4 versus the number of components (n_s). The dashed line is the linear correlation best fit

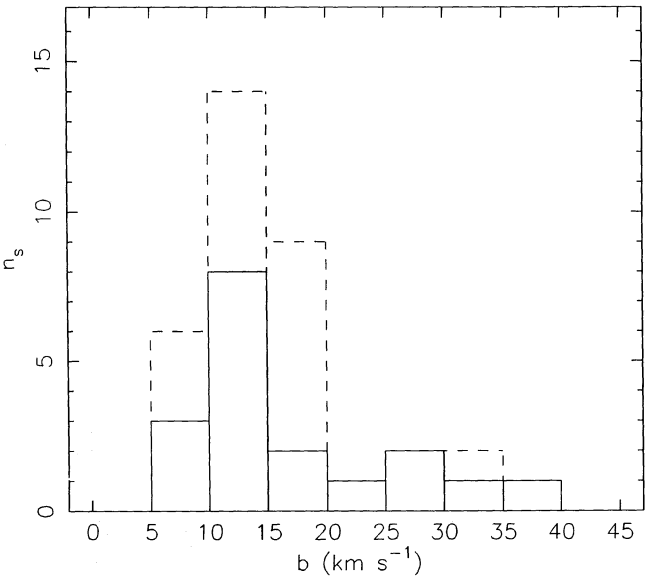

Fig. 7. Histogram of the distribution of intrinsic velocity dispersion for the subcomponents given in Table 4. The dotted part corresponds to the subsample observed at highest resolution (FWHM = 0.37 Å)

for individual clouds, some of them should have an internal velocity dispersion larger than 10 km s^{-1}. This cannot be interpreted as thermal velocities since the corresponding temperatures, in excess of 10^5 K, would imply a very high ionization level of Mg and a negligible Mg II ionic abundance. Individual clouds should then have turbulent or internal large scale motions.

If, at our resolution, we are detecting individual clouds, there should be a correlation between the Mg II λ2796 equivalent width of subcomponents and Mg II column densities. The distribution in velocity dispersion should introduce a spread in the correlation for optically thick Mg II doublets. We can infer from the distribution of velocity separations between subcomponents, discussed in the previous section, whether we have or not reached individual clouds. The number of subcomponents with velocity separations smaller than 30 km s^{-1} can be inferred from the best fit to the Δv distribution presented in Fig. 3. Normalizing this distribution to unity for Δv in the range 0–700 km s^{-1} gives a probability of 0.19 for having two clouds with $\Delta v < 30$ km s^{-1}. Thus, if the observed Δv distribution can be extrapolated to very small Δv, most of the subcomponents detected at our resolution should be individual clouds.

The Mg II λ2796 rest equivalent width of subcomponents is plotted in Fig. 8 as a function of the Mg II column density. Most of the points of w_r(Mg II λ2796) < 0.3 Å are on the linear part of the curve of growth, and the observed subcomponents, if not individual clouds, are at least optically thin Mg II entities. There are ten components with N(Mg II) > $2\,10^{13}$ cm^{-2}, all with Mg II doublet opacity larger than unity. They have velocity dispersions in the range 9 to 36 km s^{-1}, but those with $b \sim 30$ km s^{-1} could be multiple. The velocity distribution at large values of b cannot easily be derived from optically thick Mg II doublets for data at our moderate S/N ratio, and observations of weaker lines probing the same regions (at $z \sim 1$, mainly Fe II lines of small oscillator strength) would be needed to ascertain the reality of b values as large as 30 km s^{-1}.

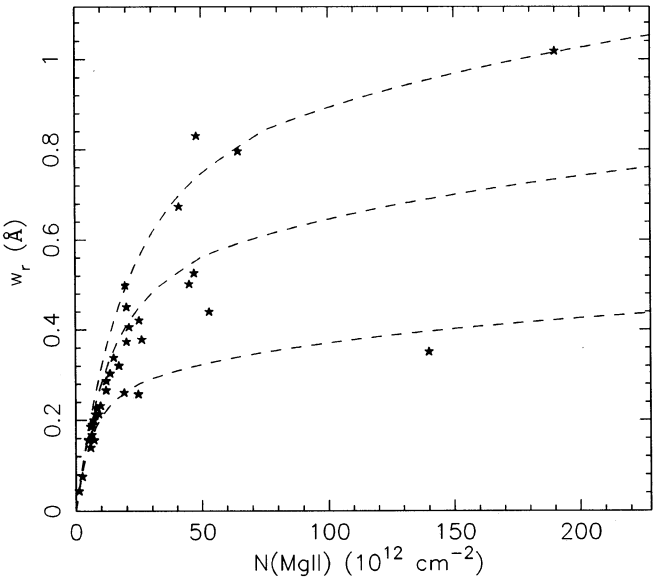

Fig. 8. Rest equivalent width of Mg II λ 2796 of each subcomponent as a function of the derived column density (in units of 10^{12} cm^{-2}). Curves of growth are plotted for velocity dispersions b of 10, 20, 30 km s^{-1} (from bottom to top). When two values of b were given in Table 4, the largest one has been used

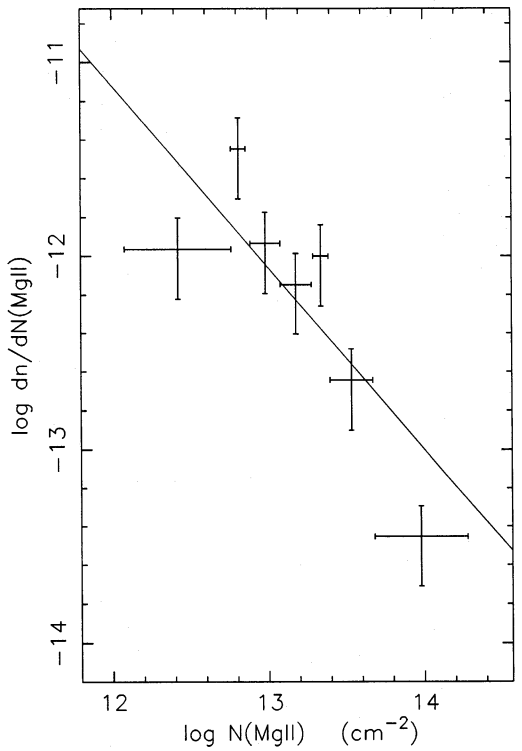

Fig. 9. The density of Mg II system per unit Mg II column density. The best fit obtained with the maximum likelihood method for a power law distribution, $dn/dN(\mathrm{Mg\,II}) \propto N(\mathrm{Mg\,II})^{-\beta}$ gives an index $\beta = 1.0 \pm 0.1$. Data have been averaged into bins only for their presentation

Let us now assume that all the subcomponents in our Mg II sample are individual clouds. We can then derive the distribution of Mg II column densities, which is given in Fig. 9. The data have been fitted by a maximum likelihood power law, $dn/dN(\mathrm{Mg\,II}) \propto N(\mathrm{Mg\,II})^{-\beta}$, with $\beta = 1.0 \pm 0.1$ for N(Mg II) in the range $1\,10^{12}$ to $2\,10^{14}$ cm^{-2}. The real distribution would be steeper if there is a large fraction of unresolved Mg II systems in our sample. This distribution should be compared with that obtained for H I column densities. There is some controversy about the shape of the N(H I) distribution: Tytler (1987) and Sargent et al. (1989) have found a single distribution for the Lyα forest and the metal-rich systems with a power law index $\beta = 1.51 \pm 0.02$ (Sargent et al. 1989), whereas Bechtold (1987) has obtained two distinct distributions, with an index $\beta = 0.8 \pm 0.1$ for $N(\mathrm{H\,I}) > 10^{16}$ cm^{-2}. Restricting their fit to higher column densities, Sargent et al. (1989) derived an index of 1.39 and commented on the discrepancy between their result and that of Bechtold (1987) as possibly due to the very large uncertainties in the N(H I) range of $3\,10^{17}$ to $3\,10^{20}$ cm^{-2}. The slope of the N(Mg II) distribution is roughly compatible with that of the N(H I) distribution found by either group. The N(Mg II) and N(H I) distributions are derived from samples with different average redshifts. Therefore, since the cosmological evolutions of Mg II and Lyman limit systems markedly differ, at least for w_r(Mg II λ 2796) > 0.6 Å (see Sect. 3), and since the ionization level of the absorbers is expected to vary with z, the N(Mg II) and N(H I) distributions are not expected to be identical.

6. Heavy element abundances

6.1. Ionic abundances

Ionic abundances are given in Table 4 for Mg I, Mg II, Fe II and Mn II. The upper limits quoted for ionic column densities are 1σ values in the optically thin case.

The Mg II column densities are in the range $1\,10^{12}$ to $2\,10^{14}$ cm^{-2}. If the H I and Mg II ions coexist in the same region, the H I column density would reach at most $6\,10^{19}$ cm^{-2} for a Mg II abundance of one tenth the solar value and no depletion onto dust grains. Results from photoionization models (Bergeron and Stasińska, 1986) with an ionization parameter $U = 10^{-3}$, 1/10 solar abundances, a power law ionizing spectrum of index $\alpha = -1.0$ and -1.5 and N(Mg II) = $2\,10^{14}$ cm^{-2} yields N(H I) = $2\,10^{20}$ and $1\,10^{20}$ cm^{-2} respectively. Heavy element abundances are poorly known, but abundances of roughly 0.1 $Z_\odot$ are within the range of current estimates for $z \leq 2$ systems (see Bergeron, 1988b). This suggests that there is probably no damped Lyα system (N(H I) > $2\,10^{20}$ cm^{-2}) in our sample. Indeed for the two systems of higher N(Mg II) (> 10^{14} cm^{-2}), $z = 0.4299$ in Q2128-123 and $z = 1.345$ in Q0215 + 015, the H I column densities derived from Lyα absorption are at most of $8\,10^{18}$ and $6\,10^{19}$ cm^{-2} respectively (Bergeron and Kunth, 1983; Blades et al., 1985).

In the case of saturated Mg II doublets, the Mg II column densities are uncertain and could be larger than the values quoted in Table 4, if velocity dispersions of individual clouds can be as small as 5 km s^{-1}. For H I column densities of the order of $1\,10^{21}$ cm^{-2} and abundances one tenth solar, the expected column density of Mn II is $3\,10^{13}$ cm^{-2}. Depletion onto grains, as observed in Galactic clouds, would lower this value by a factor of 3 to 10 (De Boer et al., 1987). In our sample there

is no detection of Mn II besides that present in the high S/N observations of Q0215 + 015, whereas in the $z = 0.436821$ cm absorption system in 3C 196 Mn II absorption lines are strong, with w_r(Mn II λ 2577) = 0.55 Å (Foltz et al., 1988). This absorber can most likely be identified with the bright, spatially resolved object 1".6 away on the sky from the quasar (Boissé and Boulade, 1989, in preparation).

The Fe II doublet $\lambda\lambda$ 2586,2600 has been observed for most systems of our sample. It is usually detected, yielding Fe II column densities very close to those of Mg II. For the system at $z = 0.4299$ towards Q2128-123, the Fe II column density has been determined using the value of b found for the Mg II doublet and the Fe II λ 2600 line equivalent width. The solar Fe/Mg abundance ratio is equal to unity, but it is only 1/20 in clouds with heavy depletion onto dust grains (De Boer et al., 1987). In photoionized models the N(Fe II)/N(Mg II) ionic ratio has similar variations with N(H I) and the ionization parameter U (ratio of the number of hydrogen ionizing photons to the product of the gas total density by the speed of light) than the N(O I)/N(C II) ionic ratio (Bergeron anf Stasińska, 1986). It is of order unity for $N(\mathrm{H\,I}) > 1\,10^{19}\,\mathrm{cm}^{-2}$ whatever $U < 0.3$, and whatever N(H I) for U of at most 10^{-4}. For $U \sim 10^{-4}$, the ratio N(C IV)/N(Mg II) is only of order 1/10 and the C IV $\lambda\lambda$ 1548,1550 doublet should be weaker than the Mg II $\lambda\lambda$ 2796,2803 absorption. There are few UV observations of C IV absorption at $z < 1$. For the absorption systems in Q0454 + 039 and Q2145 + 067, the w_r(C IV)/w_r(Mg II) equivalent width ratios equal 0.6 and 1.7 respectively (Bergeron et al., 1987). The absorber towards Q0454 + 039 has the highest N(Fe II)/N(Mg II) ionic ratio in our sample, but no detected Mn II absorption. Thus it should have an ionization parameter of the order of 10^{-3}, N(H I) in the range 10^{19}–$10^{20}\,\mathrm{cm}^{-2}$ and a small dust content. The column densities for this absorber have been computed assuming identical velocity dispersions for the Mg II and Fe II ions; relaxing this assumption, as done for the other absorbers, would lead to a somewhat higher average N(Fe II)/N(Mg II) ionic ratio.

The systems without Fe II detection do not show either Mg I absorption, and there are few Mg I detections altogether in our sample. The N(Mg I)/N(Mg II) ionic ratio is in the range $5\,10^{-3}$–$4\,10^{-2}$, and is not clearly correlated with N(Mg II) as shown in Fig. 10. The values computed by Bergeron and Stasińska (1986) for the N(Mg I)/N(Mg II) ionic ratio reach at most $1\,10^{-2}$. If N(Mg II) is not underestimated, this would suggest that the charge transfer reaction $H^+ + Mg^0$ is not as dominant over photoionization as assumed by these authors.

6.2. *The Ca II/Mg II ionic ratio*

Searches for Ca II absorption associated with Mg II systems are necessary to link properties of nearby galactic halos detected up to now only by their Ca II absorption to higher redshift absorbers.

Direct comparison between absorption lines surveys of Ca II at $z > 0.1$ and Mg II at $z \sim 0.5$ could be misleading. First, the cosmological evolution of the number per unit redshift of Mg II absorbers, at least for samples with a large equivalent width limit $w_{r,\mathrm{lim}}$(Mg II λ 2796) = 0.6 Å, could imply an increase of size with increasing redshift. Secondly, Mg and Ca differ by their abundance, depletion onto dust grains and ionization equilibrium in the presence of a UV radiation field.

There are three systems in the present survey for which the region of the expected Ca II doublet of a known Mg II absorber

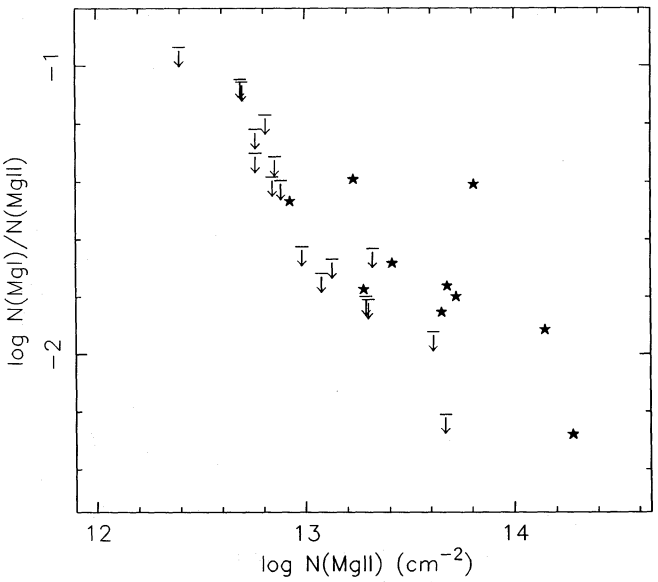

Fig. 10. The N(Mg I)/N(Mg II) column density ratio as a function of Mg II column density (in units of $10^{12}\,\mathrm{cm}^{-2}$). Upper limits are indicated as arrows

was observed. Results are described in Table 6. There is only one detection for the $z = 0.4299$ system in Q2128-123, which was already reported by Bergeron et al. (1987), and our limits for the triple $z \sim 0.36$ system in Q1101-264 are similar to those given by Robertson et al. (1988). There are altogether 4 Ca II detections, including cases published in the literature. Two are weaker than those observed for low redshift Ca II halos (see Morton et al., 1986 and references therein; Bergeron, 1988a), but the other two have rest equivalent widths for the Ca II K line well within the range (0.35 to 0.95 Å) observed for low z galactic halos. The strong Ca II absorption system at $z = 0.8366$ in Q0002-422 first reported by Boissé and Bergeron (1985) has been confirmed by Lanzetta et al. (1987). The system at $z = 0.4369$ in 3C196 has saturated Ca II lines with large equivalent widths and a doublet ratio of 1.32. It should be noted that among the 5 low redshift Ca II galactic halos, 3 are known to be 21 cm absorbers, and that one of the strong, higher redshift, Ca II absorber also shows 21 cm absorption.

In the inner parts of galactic gaseous envelopes, the H I column densities should be higher than at large radial distances and the ionization level should be lower. For the two 21 cm absorbers identified with galaxies, $z = 0.524$ in Q0235 + 164 (Smith et al., 1977) and $z = 0.4369$ in 3C196 (Boissé and Boulade, 1989, in preparation), the linear separations between the galaxy centre and the line of sight to the quasar are $9.5\,h^{-1}$ and $6.0\,h^{-1}$ kpc respectively. These projected sizes are smaller by a factor 3 to 7 than those found for the other identified Mg II absorbing galaxies (Bergeron, 1988a; Bergeron and Boissé, 1989, in preparation). For the $z = 0.524$ absorber in Q0235 + 164, only the weaker line of the Ca II doublet is detected (Cohen et al., 1987) and this ambiguous result is not included in Table 6.

At large redshift there is no evidence for the presence of dust in absorption systems with high or moderate ionization level (see e.g. Boissé and Bergeron, 1988). However a recent study of quasars with damped Lyα systems has revealed that their continuum is redder than that of quasars without high H I column

Table 6. Systems with observations of Mg II, Ca II and Fe II absorption

Quasars	z	ω_r(CaII K) (Å)	ω_r(MgII) 2796 (Å)	ω_r(MgII) 2803 (Å)	N(MgII) (cm^{-2})	b ($km\ s^{-1}$)	N(CaII) (cm^{-2})	N(FeII) (cm^{-2})	N(CaII)/N(MgII)
0002 - 422	0.8366	0.6[g]	4.7	4.0[d]	$1.6\ 10^{16}$[d]	49 & 71[d]	$> 6.6\ 10^{12}$[c]	$8\ 10^{14}$[d]	$> 4.1\ 10^{-4}$
0302 - 223	0.4196	< 0.09[i]	0.9[j]	0.8[j]					
0454 - 220	0.4744	0.13[e]	1.37	1.34[e]	$3.0\ 10^{15}$[e]	30[e]	$1.6\ 10^{12}$[e]	$8.\ 10^{14}$[e]	$5.3\ 10^{-4}$
0735 + 178	0.4241	< 0.06[e]	1.32	1.02[h]	$9.6\ 10^{13}$[h]		$< 7.5\ 10^{11}$[e]	$1.2\ 10^{14}$[e]	$< 7.8\ 10^{-3}$
0809 + 483	0.4369	0.54[k]	2.00[k]	1.88[k]	$2.5\ 10^{15}$:	33	$> 5.9\ 10^{12}$[c]		$> 2.4\ 10^{-3}$
1101 - 264	0.3564	< 0.035[i]	0.22	0.19[f]	$1.0\ 10^{13}$	5 & 11[f]	$< 4.0\ 10^{11}$[c]		$< 6.3\ 10^{-2}$
	0.35903	< 0.035[i]	0.25	0.21[f]	$2.5\ 10^{13}$	9[f]	$< 4.0\ 10^{11}$[c]	$> 8\ 10^{12}$	$< 1.6\ 10^{-2}$
	0.35923	< 0.035[i]	0.24	0.19[f]	$1.2\ 10^{13}$	14[f]	$< 4.0\ 10^{11}$[c]	$> 2.5\ 10^{12}$	$< 3.3\ 10^{-2}$
2128 - 123	0.4299	0.10[i]	0.41	0.37[i]	$1.4\ 10^{14}$[a]	8.6[a]	$2.6\ 10^{12}$[b]	$1.9\ 10^{14}$[b]	$1.9\ 10^{-2}$

[a] Doublet ratio method
[b] Using b (Mg II)
[c] Optically thin case
References : [d] Sargent et al. (1980), [e] Robertson et al. (1988), [f] Carswell et al. (1984), [g] Boissé and Bergeron (1985), [h] Boksenberg et al. (1979), [i] this work, [j] Bergeron (unpublished), [k] Foltz et al. (1988)

density absorption line systems, which is best explained by extinction from dust in the absorbers (Fall et al., 1989). These systems are of low ionization level, usually show 21 cm absorption and can possibly be identified with protogalactic disks (Wolfe et al., 1986; Wolfe, 1988).

Galactic halos at lower redshift should have similar properties, and dust is more likely to be present in the 21 cm absorbers. At large radial distance from the nucleus, the Ca II ionic abundance should be dominated by ionization equilibrium and not by depletion onto dust grains. When strong C IV absorption is detected, as mentioned in Sect 6.1 for two cases of our sample, Ca III is expected to be the dominant ion. If no UV data are available, the Mg II/Fe II ionic ratio can be used to evaluate the H I column density and to constrain the ionization level (see Sect 6.1). The Ca II ion should be a minority species when the N(Mg II)/N(Fe II) ionic ratio is much larger than unity, both Fe and Ca being then essentially doubly ionized. In 21 cm absorption systems, Mg II and Ca II should coexist with the H I phase and the N(Ca II)/N(Mg II) ionic ratio should give an estimate of the Ca depletion onto dust grains. Unfortunately in these cases the Mg II and Fe II absorption lines are usually heavily saturated and their column densities are very uncertain. This obviously applies to the $z = 0.4369$ absorber in 3C196. It is then better to compare the Ca II ionic abundance to that of a trace element with a much smaller depletion factor onto dust; for $z \sim 0.5$ absorption systems, only Mn II can be observed in the optical.

Toward ζ Oph, the observed N(Mn II)/N(Ca II) ionic ratio equals 40 (Morton, 1978), whereas the Mn/Ca relative solar abundance is 0.13, which gives a depletion of Ca relative to Mn of 300. We have estimated the Mn II and Ca II column densities in the $z = 0.4369$ system in 3C196, using the equivalent widths measured by Foltz et al. (1988) and the doublet ratio method. We get $N(\mathrm{Mn\ II}) = 5.5\ 10^{13}\ \mathrm{cm}^{-2}$ and $N(\mathrm{Ca\ II}) = 1.9\ 10^{13}\ \mathrm{cm}^{-2}$, which gives a depletion of Ca relative to Mn of 22 and thus implies the presence of a large amount of dust in this 21 cm absorber. Optical observations at higher spectral resolution are needed to obtain a more accurate determination of depletion factors since this system could be multiple.

7. Conclusion

We have presented in the previous sections evidence for a variation in the cosmological evolution of the density of Mg II systems as a function of the rest equivalent width limit of the Mg II samples. This implies a decreasing fraction of small to strong Mg II systems with increasing redshift.

There is a strong evolution with redshift of the number of Mg II systems for samples with an equivalent width limit $w_{r,\min}$ (Mg II λ 2796) = 0.6 Å. This evolution must weaken with decreasing values of $w_{r,\min}$, and for samples with $w_{r,\min}$(Mg II λ 2796) = 0.2 to 0.3 Å the redshift distribution of the Mg II absorbers should be consistent with a non evolving population (for Friedmann cosmology with $q_0 = 0$ or 0.5), as this is the case for Lyman limit systems. An independent analysis of Caulet (1989) leads to the same conclusion.

The redshift dependence of the evolution of the density per unit redshift of large Mg II systems is $(1+z)^\gamma$ with $\gamma \sim 2.0$ (Tytler et al., 1987; Boulade et al., 1987). This corresponds to an increase of the product of the space density of these absorbers by their projected cross-section by a factor of 5.2 for the redshift interval 0 to 2 and $q_0 = 0.5$. The other population which shows a strong evolution with redshift is the damped Lyα systems if, following Wolfe (1988), these absorbers are assumed to be protogalactic disks. The sizes of the damped Lyα systems can be inferred from their density per unit redshift and from the properties of nearby H I disks (Wolfe et al., 1986; Turnshek et al., 1989). This size exceeds that of $z \sim 0$ H I disks by a factor 2.5 to 3 at $z = 2.2$. Consequently, strong Mg II absorbers and damped Lyα systems have both a strong evolution with redshift of the product of their covolumic space density by their projected cross-section. Thus the cross-section of gaseous regions with high density and/or high column density should strongly increase with increasing redshift in the range $z = 0$-2.5, whereas the overall size of the gaseous halo, as probed by the LLS, is non evolving. Alternatively the covolumic space density of dense gaseous regions could increase with redshift. These dense zones could then still be embedded in a more diffuse very extended gaseous envelope.

Another striking property of the Mg II absorbers relates to line multiplicity. It has already been suggested that the sequence in C IV line strength is a sequence in velocity separation of multiple components (Wolfe, 1986; York et al., 1986). For the Mg II systems we have found a strong correlation between the line equivalent width and the number of subcomponents. Thus for both low z Mg II and high z C IV systems, the line strength is essentially a measure of the number of individual clouds encountered on a linepath, and not of their column density. This property should not apply to the damped Lyα population.

Most of the Mg II subcomponents found at our spectral resolution have a Mg II doublet of moderate opacity. These absorbers with typically $N(\mathrm{Mg\,II}) \sim 10^{13}\,\mathrm{cm}^{-2}$ must then have velocity dispersions larger than $b = 10\,\mathrm{km\,s}^{-1}$. Turbulent components with large velocity dispersion ($\sim 50\,\mathrm{km\,s}^{-1}$) have indeed been found in some 21 cm absorbers (see e.g. Foltz et al., 1988). These subcomponents can cluster in some cases around highly optically thick ones. The distribution of Mg II column densities for the observed subcomponents can be fitted by a power law $dn/dN(\mathrm{Mg\,II}) \propto N(\mathrm{Mg\,II})^{-\beta}$ with $\beta = 1.0 \pm 0.1$.

We can infer whether these low $N(\mathrm{Mg\,II})$ components exist at $z \sim 2$ by estimating their associated C II λ 1334 absorption. The C II ions are always the dominant species when the Mg II/Mg ionic ratio is large (Bergeron and Stasińska, 1986). The C II/Mg II ionic ratio roughly equals the C/Mg abundance ratio for $N(\mathrm{H\,I}) > 10^{19}\,\mathrm{cm}^{-2}$ and could take even higher values for $N(\mathrm{H\,I}) < 10^{19}\,\mathrm{cm}^{-2}$. Thus a $w_r(\mathrm{Mg\,II}\,\lambda 2796) = 0.2$ Å absorption should be associated with a C II λ 1334 absorption of higher w_r as the smaller oscillator strength of the latter (by a factor of 5) is by far compensated by the value of the C II/Mg II ionic ratio which equals at least 20. At $z \sim 2$, C II absorption is not detected in C IV systems of moderate strength and it is usually strong when present (see e.g. the C IV survey of Sargent et al., 1988b). This also follows from the trend of increasing $w_r(\mathrm{Mg\,II}\,\lambda 2796)$ with increasing $w_r(\mathrm{Mg\,II})/w_r(\mathrm{C\,IV})$ equivalent width ratio suggested by Bergeron and Boissé (1984) and confirmed by Lanzetta et al. (1987). Weak Mg II systems should then be rare at $z \sim 2$, whereas weak C IV absorbers, down to $w_{r,\min}(\mathrm{C\,IV}\,\lambda 1548) = 0.15$ Å (Sargent et al., 1988b) are the dominant population and exceed the LLS in number by a factor 1.6.

This evolution in the relative number of weak to strong Mg II systems, together with the disappearance of weak Mg II absorbers at $z \sim 2$ should result in a strong evolution with z of the multiplicity of Mg II systems, as also suggested by Lanzetta (1988).

To properly study the evolution of the absorbing components of lower density and/or smaller column density, it is probably necessary to combine properties of low z, weak Mg II systems with those of $z \sim 2$, weak C IV systems. The parts of the gaseous halos, sampled by these two types of systems at different redshifts, would then have an ionization level increasing with redshift for $0 < z < 2.5$.

Clustering of Mg II systems at $z \sim 1$ is important as revealed by the frequent line splitting. The two-point correlation function for the Mg II redshifts shows a significant excess at velocity separations less than $200\,\mathrm{km\,s}^{-1}$, as also observed by Sargent et al. (1988a), but also up to $600\,\mathrm{km\,s}^{-1}$. The distribution of velocity separations is best fitted by two Gaussian components with dispersions of 80 and $390\,\mathrm{km\,s}^{-1}$. The component of larger velocity dispersion can be due to relative motions between field galaxy pairs, if the distribution of relative velocities observed for local galaxies prevails at $z \sim 1$. Velocity distributions of galaxies in clusters have dispersions larger by a factor of about 2.5. This explanation is consistent with identifications of Mg II absorbers mainly with field galaxies (Bergeron, 1988b).

Modelling the expected number of clouds per line of sight and their maximum velocity separation, in the assumption of a spherical or disklike geometry, also favors two distinct populations for the two components of the velocity separation distribution. A single population with a two velocity component model reproduces adequately the number of observed Mg II subcomponents but not their maximum velocity separation.

The distribution of Mg II velocity separations should be compared with that of C IV systems at $z \sim 2$. Unfortunately our Mg II sample is too small to give information on velocity scales larger than $700\,\mathrm{km\,s}^{-1}$ and on the level of the Poissonian background, and the much larger C IV sample of Sargent et al. (1988b) gives splitting only on scales larger than $200\,\mathrm{km\,s}^{-1}$. The two-point correlation for the C IV redshifts appears to cut-off at $\Delta v \sim 600\,\mathrm{km\,s}^{-1}$, with possibly some structures on larger velocity scales. It is not clear whether this cut-off is related to our broader distribution of velocity separations.

Abundances of heavy elements cannot be estimated when the H I column density and the ionization level of the absorber are unknown, which is nearly always the case for $z < 1.2$ absorbers. Relative abundances of some heavy elements could be determined, if the observed ions coexist in the same phase and are the dominant species. This is true for singly ionized elements, such as Mg II, Ca II and Fe II, only if the H I column density is larger than $3\,10^{19}\,\mathrm{cm}^{-2}$ (Bergeron and Stasińska, 1986). Since no damped Lyα system is known at low z, the likely candidates are 21 cm absorbers, assuming that the linepaths to the quasar optical and radio sources cross the same absorber. The H I column density on the optical path should then be larger than about $10^{20}\,\mathrm{cm}^{-2}$ and the dominant species should be singly ionized ions for most heavy element. For abundances of about one tenth solar, as determined for some systems (see e.g. Bergeron and D'Odorico, 1986), the Mg II doublet and most Fe II absorption lines should be heavily saturated and the derived Mg II and Fe II column densities are uncertain. Reliable abundances can be determined only for elements of smaller abundance than Mg and Fe, or for elements depleted onto dust grains. For $z < 1$ absorption systems Mn and Ca are the two elements observable in the optical. At higher redshift, Ni, Cr and Zn are observable (Meyer and York, 1987; Pettini et al., 1990; Meyer et al., 1989).

The depletion of Ca relative to Mn is very large: it reaches 300 towards ζ Oph (Morton, 1978). The $N(\mathrm{Mn\,II})/N(\mathrm{Ca\,II})$ ionic ratio can thus probe the presence of dust in low redshift 21 cm absorbers. Using the data obtained by Foltz et al. (1988) for the $z = 0.4369$ system in 3C196, we find a depletion of Ca relative to Mn of 22, which implies a large amount of dust in this absorber. A similar analysis on high spectral resolution data for the few low redshift 21 cm absorbers, compared to that for Cr or Ni (large depletion factors in the Galactic interstellar medium) and Zn (not depleted) in high redshift damped Lyα absorbers will give the evolution with redshift of the dust content in high $N(\mathrm{H\,I})$ column density absorbers.

Acknowledgements. We are deeply indebted to A. Boksenberg for making the IPCS observations possible. We also thank P. Boissé for fruitful discussions.

References

Bechtold, J.: 1987, in *High Redshift and Primeval Galaxies*, eds. J. Bergeron, D. Kunth, B. Rocca-Volmerange, Editions Frontières, Paris

Bechtold., J., Green, R.F., Weymann, R.J., Schmidt, M., Estabrook, F.B., Sherman, R.D., Wahlquist, H.D., Heckman, J.M.: 1984, *Astrophys. J.* **281**, 76

Bergeron, J.: 1986, *Astron. Astrophys. Letters* **155**, L8

Bergeron, J.: 1988a, IAU Symposium No. 130, eds. J. Audouze, M.C. Pelletan, A. Szalay, Kluwer, Dordrecht, p. 343

Bergeron, J.: 1988b, in *QSO absorbing lines: Probing the universe*, eds. J.C. Blades, D.A. Turnshek, C.A. Norman, Cambridge University Press, Cambridge, p. 127

Bergeron, J., Boissé, P.: 1984, *Astron. Astrophys.* **133**, 374

Bergeron, J., D'Odorico, S.: 1986, *Monthly Notices Roy. Astron. Soc.* **220**, 833

Bergeron, J., D'Odorico, S., Kunth, D.: 1987, *Astron. Astrophys.* **180**, 1

Bergeron, J., Kunth, D.: 1983, *Monthly Notices Roy. Astron. Soc.* **205**, 1053

Bergeron, J., Savage, B., Green, R.F.: 1987, in *The Scientific Accomplishments of the IUE*, ed. Y. Kondon, Reidel, Dordrecht, p. 703

Bergeron, J., Stasińska, G.: 1986, *Astron. Astrophys.* **169**, 1

Blades, J.C., Hunstead, R.W., Murdoch, H.S., Pettini, M.: 1985, *Astrophys. J.* **288**, 580

Boissé, P., Bergeron, J.: 1985, *Astron. Astrophys.* **145**, 59

Boissé, P., Bergeron, J.: 1988, *Astron. Astrophys.* **192**, 1

Boksenberg, A., Carswell, R.F., Sargent, W.L.W.: 1979, *Astrophys. J.* **227**, 370

Boulade, O., Kunth, D., Tytler, D., Vigroux, L.: 1987, in *High Redshift and Primeval Galaxies*, eds. J. Bergeron, D. Kunth, B. Rocca-Volmerange, Editions Frontières, Paris, p. 349

Carswell, R.F., Morton, D.C., Smith, M.G., Stockton, A.N., Turnshek, D.A., Weymann, R.J.: 1984, *Astrophys. J.* **278**, 486

Caulet, A.: 1989, *Astrophys. J.* **340**, 90

Cohen, R.D., Smith, H.E., Junkkarinen, V.T., Burbidge, E.M.: 1987, *Astrophys. J.* **318**, 577

Davis, M., Peebles, P.J.E.: 1983, *Astrophys. J.* **267**, 465

De Boer, K.S., Jura, M.A., Shull, J.M.: 1987, *The Scientific Accomplishments of the IUE*, ed. Y. Kondon, Reidel, Dordrecht, p. 485

De Lapparent, V., Geller, M.J., Huchra, J.P.: 1988, *Astrophys. J.* **332**, 44

D'Odorico, S., Pettini, M., Ponz, D.: 1985, *Astrophys. J.* **299**, 852

Fall, S.M., Pei, Y.C., McMahon, R.G.: 1989, *Astrophys. J. Letters* **345**, L5

Foltz, C.B., Chaffee, F.H. Jr., Wolfe, A.M.: 1988, *Astrophys. J.* **335**, 35

Geller, M.: 1987, in *Large Scale Structure in the Universe*, Saas Fee lectures, ed. L. Martinet

Lanzetta, K.M. 1988, *Astrophys. J.* **332**, 96

Lanzetta, K.M., Turnshek, D.A., Wolfe A.M.: 1987, *Astrophys. J.* **322**, 739

Meyer, D.M., York, D.G.: 1987, *Astrophys. J. Letters* **319**, L45

Meyer, D.M., Welty, D.E., York, D.G.: 1989, *Astrophys. J. Letters* **343**, L37

Morton, D.C.: 1978, *Astrophys. J.* **222**, 863

Morton, D.C., York, D.G., Jenkins, E.B.: 1986, *Astrophys. J.* **302**, 272

Morton, D.C., York, D.G., Jenkins, E.B.: 1988, *Astrophys. J. Suppl.* **68**, 449

Pelat, D., Alloin, D.: 1980, *Astron. Astrophys.* **81**, 172

Pettini, M., Boksenberg, A., Hunstead, R.W.: 1990, *Astrophys. J.* **348**, 48

Robertson, J.G., Morton, D.C., Blades, J.C., York, D.G., Meyer, D.M.: 1988, *Astrophys. J.* **325**, 635

Sargent, W.L.W., Steidel, C.C., Boksenberg, A.: 1988a, *Astrophys. J.* **334**, 22

Sargent, W.L.W., Boksenberg, A., Steidel, C.C.: 1988b, *Astrophys. J. Suppl.* **68**, 539

Sargent, W.L.W., Steidel, C.C., Boksenberg, A.: 1989, *Astrophys. J. Suppl.* **69**, 703

Sargent, W.L.W., Young, P.J., Boksenberg, A., Tytler, D.: 1980, *Astrophys. J. Suppl.* **42**, 41

Smith, H.E., Burbidge, E.M., Sunkkarinen, V.T.: 1977, *Astrophys. J.* **218**, 611

Tully, R.B., Shaya, E.J.: 1984, *Astrophys. J.* **281**, 31

Turnshek, D.A., Wolfe, A.M., Lanzetta, K.M., Briggs, F.H., Cohen, R.D., Foltz, C.B., Smith, H.E., Wilkes, B.J.: 1989, *Astrophys. J.* **344**, 567

Tytler, D.: 1982, *Nature* **298**, 427

Tytler, D., Boksenberg, A., Sargent, W.L.W., Young, P., Kunth, D.: 1987, *Astrophys. J. Suppl.* **64**, 667

York, D.G., Dopita, M., Green, R., Bechtold, J.: 1986, *Astrophys. J.* **311**, 610

Young, P.J., Sargent, W.L.W., Boksenberg, A.: 1982, *Astrophys. J. Suppl.* **48**, 455

Weymann, R.J., Williams, R.E., Peterson, B.M., Turnshek, D.A.: 1979, *Astrophys. J.* **234**, 33

Wolfe, A.M.: 1986, in *Proc. NRAO Conf. on Gaseous Halos of Galaxies*, eds. J. Bregman, J. Lockman, NRAO SP, p. 259

Wolfe, A.M.: 1988, in *QSO absorbing lines: Probing the universe*, eds. J.C. Blades, D.A. Turnshek, C.A. Norman, Cambridge University Press, Cambridge, p. 297